MANSOURA JOURNAL OF CHEMISTRY
Official Journal of Faculty of Science, Mansoura University, Egypt
E-mail: scimag@mans.edu.eg ISSN: 2974-4938

Designing of NiO/NiS_2@ nitrogen-doped carbon for high-performance hybrid supercapacitor

Omnya Mustafa[a*], Doaa A. Kospa[a], Ahmed Gebreil[b], Amr Awad Ibrahim[a]*

[a] *Department of Chemistry, Faculty of Science, Mansoura University, Al-Mansoura 35516, Egypt.*

[b] *Nile Higher Institutes of Engineering and Technology, El-Mansoura, Egypt.)*

**** Correspondence to:** omnyamostafa873@gmail.com, 01063576215*

Received: 21/9/2025
Accepted:12/10/2025

Abstract: High-performance energy storage devices are required as consumer electronics, electric vehicles, and smart meters grow at a rapid pace. Supercapacitors are currently considered one of the highly promising energy devices for upcoming energy technologies. Herein, NiO/NiS_2@nitrogen doped carbon composite was used as a hybrid supercapacitor electrode. Several techniques, including scanning electron microscopy (SEM) and transmission electron microscopy (TEM), were applied to evaluate the interfacial properties and structure of the as-synthesized NiO/NiS_2@NC.Moreover, X-ray diffraction (XRD) confirmed the synthesis of NiO and NiS_2 crystalline phases with a distinct carbon peak at 2θ=23° that revealed the formation of NiO/NiS_2 over N-doped carbon. Interestingly, the synergetic interaction between NiS_2 and NiO enhances conductivity and electrochemical performance, while nitrogen-doped carbon significantly boosts surface area and specific capacitance. The electrochemical characteristics were thoroughly investigated in a 3 M KOH solution by using the techniques of cyclic voltammetry (CV) and the galvanostatic charge-discharge (GCD) approach. NiO/NiS_2@NC has enhanced electrochemical performance, obtaining a specific capacitance of 1134 F g^{-1} at 1 A g^{-1}, whereas NC reaches 369 F g^{-1} under comparable current density conditions.

Keywords: Polyacrylamide, nitrogen-doped carbon, electrochemical supercapacitor.

1. Introduction

The growing depletion of energy from fossil fuels, coupled with concerns about accelerated global warming linked to fossil fuel consumption, requires the urgent exploration of renewable energy alternatives, including wind, tidal, and solar energy.[1, 2] Nonetheless, the mentioned renewable energy sources face sustainability challenges and are constrained by temporal or regional factors; an electrochemical energy storage system is needed to attain their practical application.[3] Consequently, Significant advancements have been observed in the realm of energy storage devices, which have attracted interest as a feasible approach to address pressing issues related to the heavy reliance on fossil fuels. Amongst these energy storage technologies, supercapacitors (SCs) have garnered considerable attention as promising storage solutions,[4] due to they possess high capacitance, extended cycle life, rapid charge-discharge rates, minimal environmental effect, and outstanding cycling performance.[5, 6] SCs are commonly classified into three basic types: pseudocapacitors(PCs), hybrid supercapacitors (HSCs), and electric double-layer capacitors (EDCLs), which differ in their electrochemical energy storage process.

PCs exhibit remarkable charge storage capabilities and facilitate rapid, reversible faradic reactions occurring at the interface of active materials. EDLCs exhibit a notably reduced capacity in comparison to Pseudocapacitors. The reliability of PCs declines due to the breakdown of the active material's structure.[7, 8] Moreover, hybrid supercapacitors are considered effective in energy storage due to their elevated specific energy capacity, which is attained by combining high voltage with the complementary features of EDLC and PCs.

Nonetheless, HSCs provide extraordinary electrical power and exceptional cycle stability, making them very suitable for a variety of energy storage applications.[7]

A variety of initiatives have been undertaken, such as the development and construction of hierarchical structures, the synthesis of materials aimed at current collectors, the application of dopants, and the preparation of conducting polymers (CPs) to improve the capacitance of SCs.[8-10] N-doped carbon produced from conducting polymers and metal sulfides has garnered significant attention as electrode materials for supercapacitors to meet the energy demands of portable devices and renewable energy storage applications.[11]

In recent years, there has been extensive investigation and application of transition-metal oxides and sulfides with diverse chemical valence states as electrode materials for supercapacitors.[12] NiO stands out among them because it is inexpensive, exhibits clear redox behavior, has a high theoretical specific capacitance, and is environmentally friendly.[13] Nonetheless, the actual specific capacitance of NiO is significantly inferior to its theoretical value due to elevated charge-transfer resistance; this reduction continues to pose a substantial hurdle for its practical application.[14] To tackle this issue, efforts have been made to enhance the performance of NiO by incorporating it with carbon-based conductive materials, like graphene and carbon nanotubes. They also used transition-metal sulfides, particularly nickel sulfides, in the NiO system, as nickel sulfides possess greater crystal lattice dimensions and a narrower band gap compared to NiO.[15] These differences alter electron transfer rates, leading to faster and reversible redox processes, lower charge-transfer resistance, and higher conductivity.

The composition has significant effects on the electrochemical characteristics of the SC substance. In the context of carbon nanomaterials, the introduction of heteroatoms, like nitrogen, enhances the electrochemical activity of the product.[16] Doping of heteroatoms such as nitrogen into the carbon structure modifies the electron distribution among adjacent carbon atoms, leading to the creation of an active site that contains nitrogen in nitrogen-doped carbon (NCs). Post-treatment, in-situ doping, and carbonization are prevalent methods for integrating nitrogen into the carbon framework.[17] Nonetheless, the intrinsic limitations, including the time-intensive nature, the production of hazardous gaseous byproducts (NH_3), and the elevated complexity associated with in-situ doping and post-processing, have constrained their application. Consequently, direct carbonization has surfaced as an uncomplicated method for producing N-doped carbon compounds and has been the focus of extensive investigation.[18] The materials that can serve as precursors for direct carbonization may encompass synthetic polymers, including polypyrrole, polyaniline, polyacrylamide and polyacrylonitrile.[19, 20] Polyacrylamide (PAM) is a polymer characterized by its richness in nitrogen and carbon, which can undergo carbonization and subsequently establish a conductive network, thereby improving the stability and electrical conductivity of materials.[21] In this study, we developed a cheap and efficient synthesis technique of nitrogen-doped carbon using crosslinked polyacrylamide gel as a carbon and nitrogen source with nickel sulfide that was formed by facile hydrothermal followed by a carbonization process. For novel NiO/NiS_2 @NC, the presence of N-doped carbon derived from polyacrylamide provides a high surface area and facilitates electron transfer. Moreover, the synergetic effect between nickel sulfide and nickel oxide provides rich redox sites. This distinctive combination yields improved conductivity, reliability of structure, and electrochemical performance in comparison with the conventional NiO/NiS_2 electrode. The catalytic behaviors of NiO/NiS_2 @NC were explored in a KOH electrolyte (3 M) by adopting SCs as a benchmarked system. The results demonstrate that NiO/NiS_2 @NC displays outstanding specific capacitance (1134 F g^{-1} at 1 A g^{-1}), compared to NC, which has 369 F g^{-1} at the same current density.

2. Materials and methods

2.1. Materials and chemicals

Every chemical used was sourced from a commercial source without any further purification. Acrylamide (AAm), ammonium persulfate (APS), nickel chloride hexahydrate

($NiCl_2.6H_2O$), potassium hydroxide (KOH), hydrochloric acid (HCl), N, N -methylene bisacrylamide(MBA), ethanol (C_2H_5OH), acetone (C_3H_6O), and distilled water were used to prepare all aqueous solutions.

2.2. Synthesis of NiS_2

NiS_2 was synthesized utilizing a simple hydrothermal technique. To begin, 1 M of $NiCl_2 \cdot 6H_2O$ and 3 M of Na_2S were dissolved in 100 mL of distilled water and stirred vigorously for 4 hours. The homogeneous solution was put into a 200 mL Teflon autoclave, subjected to a temperature of 140 °C for 20 hrs. The autoclave was then permitted to cool naturally. The lightly colored precipitates were gathered through filtration and subsequently rinsed with water and acetone several times before being dried in a vacuum oven at 65 °C for 18 hours.[22]

2.3. Synthesis of NiO/NiS_2 @NC

Firstly, 2.0 g of acrylamide was dissolved in 25 mL of distilled water. After that, 0.5 g of NiS_2 was added to the previous solution under stirring for 15 min. Then, while stirring constantly, 0.025 g of MBA was added for 10 min. Subsequently, 0.1 g of APS was dissolved in the previous mixture with continuous stirring for another 10 min then transferred to the oven at 80 °C for 1 hr or till gelation. After that, nickel sulfide incorporated with hydrogel was obtained and washed three times by distilled water, then dried overnight and ground to small particles in mortar. Finally**,** the ground particles were calcined in a muffle at 700 °C for 2 hours at a rate of 5 °C min^{-1} to obtain NiO/NiS_2@NC**.** Pure nitrogen-doped carbon can be synthesized using the aforementioned processes in the absence of nickel sulfide.

2.3.1 The mechanism of production of NiS_2

The first step to producing NiS_2 is when Ni^{2+} reacts with S^{2-} ions to form NiS intermediates. These intermediates are then turned into NiS_2 in the presence of extra sulfur species and under hydrothermal conditions. The total reaction is.

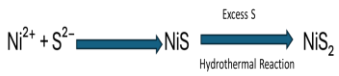

2.4. Material Characterization

Diverse techniques were utilized to ascertain the efficacy of the product. SEM (JEOL JSM 6510LV) was used to detect chemical composition and morphologies. A transmission electron microscope (JEOL JEM-2200FS) was utilized to investigate the morphology of the as-synthesized catalysts. The X-ray powder diffraction (XRD) patterns of the nanocomposites were obtained using Cu K_a radiation (λ=1.5406Å, Bruker D8 ADVANCE). The catalysts were electrochemically analyzed using Corrtest CS350, and then the resulting data were fitted with CS workstation software.

2.5. Electrochemical Performances

Electrochemical studies were performed using a *Corrtest CS350* workstation. The preparation of the working electrode involved the combination of 80 wt% active material (NiO/NiS_2@NC), 10 wt% acetylene black, and 10 wt% polyvinylidene fluoride to create a slurry. Subsequently, the slurry was applied to Ni foam (1x1 cm^2) and dried at 80 °C overnight. Electrochemical measurements started with the cyclic voltammetry (CV), then galvanostatic charge-discharge (GCD) was applied at different current densities. Finally, an electrochemical impedance spectrum (EIS) was conducted with a 5 mV amplitude across a frequency range of 0.1 Hz to 100 kHz. All measurements were carried out in a standard three-electrode configuration in a 3 M KOH solution. Platinum sheets and Ag/AgCl (KCl, saturated) were utilized as reference and auxiliary electrodes. The capacitance is generally calculated using the equation provided below:

$$\mathbf{C_s} = \frac{\boldsymbol{I\,\Delta t}}{\boldsymbol{m\,\Delta V}} \qquad \textbf{(1)}$$

C_s, I, Δt, m, and ΔV represent the specific capacitance (F/g), current at the discharge (A), discharge duration (s), specific mass (g) of the material in use, and voltage variation (V), respectively.

3. Results and Discussion

3.1. Specifications of the Materia

XRD was applied to verify the structure and phase composition of the (NiO/NiS_2 @NC).

Fig. 1(a) displays the XRD pattern of NiO/NiS_2 @NC. The diffraction peaks of the composite can be observed at 2θ = 31.7° and 45.5 °, which are attributed to (200) and (220) planes of NiS_2 (JCPDS No.89-3058).[23] In addition, peaks at 2θ = 19.2° and 32.3°are

assigned to the (001)and (300) planes of NiS phase (JCPDS No. 86-2281) that formed due to the decomposition of NiS_2 at high calcination temperatures to a hybridized structure of NiS_2/NiS.[24, 25] Furthermore, the peaks at 2θ = 37.3°, 43.4°, 63°, 75.7°, and 79.8°, which are related to (111),(200),(220),(311), and (222) planes of NiO peaks (JCPDS:65-5745). The sharp intensity of these peaks confirmed

domination of NiO in the sample.[26] Notably, peaks at 2θ = 28.4° and 29.4° correspond to (311) and (313) planes of an excess of sulfur.[27]The peak at 2θ=23° was attributed to the (002) plane of graphite, which confirmed the synthesis of N-doped carbon.

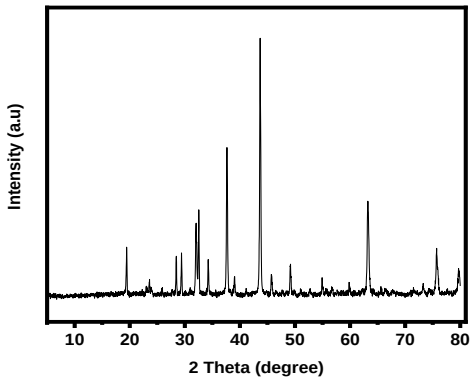

Fig.1: (a) XRD patterns of NiO/NiS_2@NC

The structure and surface morphology have been evaluated by SEM and TEM. As shown in Fig. 2a, the SEM image revealed that NiO/NiS_2@NC particles have the spherical shape of NiO, confirming the overwhelming presence of NiO, which matched the XRD result. In addition, the TEM micrograph clearly indicates that the nanoparticles are virtually uniform in size, with a spherical shape of NiO.

3.2. Electrochemical performance of NiO/NiS_2 @NC.

Fig. 3 illustrates the cyclic voltammetry curves in a 3 M KOH electrolyte, for NiO/NiS_2@NC and NC across a potential range of (0.0- 0.45 V) with a scan rate of 10 mV/s. Each electrode exhibits a pair of redox peaks, suggestive of faradaic pseudocapacitive behaviour. Interestingly, the NiO/NiS_2@NC electrode possesses the largest integrated CV curve area and the greatest current peak, consistent with its enhanced morphological and structural attributes.

GCD curves (Fig. 3b) demonstrate that the discharging time of the NiO/NiS2@NC is notably extended, leading to enhanced capacitance values, which align with its CV results. The excellent symmetry of the GCD curves implies superior electrochemical reversibility and Coulombic efficiency. Moreover, different current densities, ranging from 1 to 10 A g^{-1}, were applied to NiO/NiS_2@NC and NC, as shown in (Fig. 3c – d).

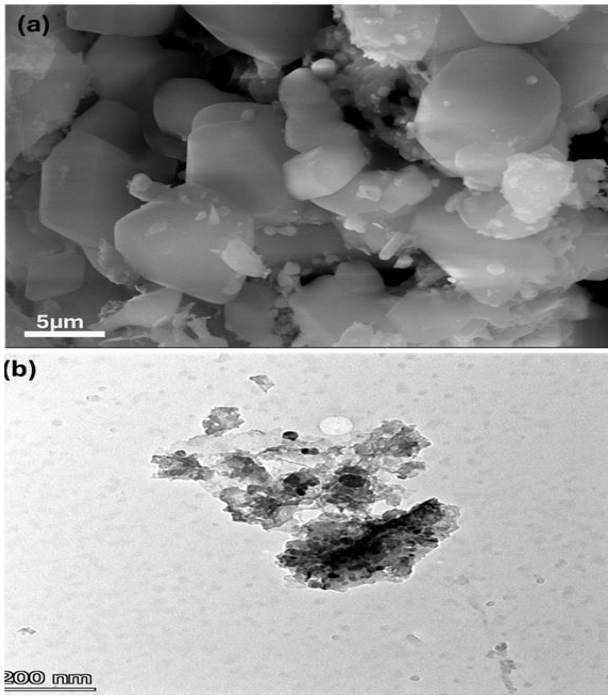

Fig. 2: (a) SEM and (b) TEM of NiO/NiS_2@NC.

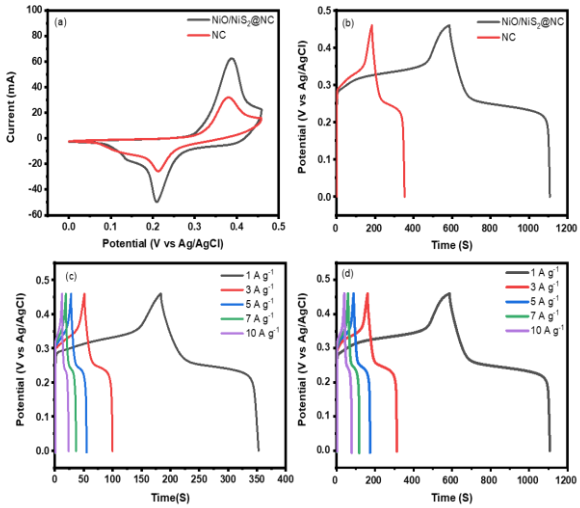

Fig. 3: (a) Cyclic voltammetry curves of NiO/NiS_2@NC and NC at 10 mV s^{-1}, (b) GCD plots of NiO/NiS_2@NC and NC at 1 A g^{-1}, GCD at different current densities of (c) NC and (d) NiO/NiS_2@NC.

Fig.4 exhibts the specific capacitances of NC and NiO/NiS_2@NC electrodes from 1 to 10 A g^{-1} using GCD (Eq.1). The figure indicates that the NiO/NiS_2@NC electrode has a larger capacitance than the NC electrode. At 1, 3, 5, 7, and 10 A g^{-1}, the specific capacitances of the NiO/NiS_2@NC electrode are 1134, 978, 923, 882, and 717 F g^{-1}, respectively, which are greater than those of the NC electrode (369, 319, 282, 258, and 250 F g^{-1}).

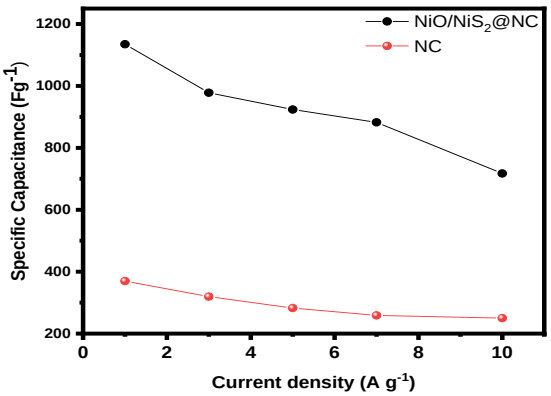

Fig. 4: Coulombic efficiency at different current densities of NC and NiO/NiS_2@NC

EIS is commonly used to study the electrolyte ion transport characteristics of electrode materials for SCs. The Nyquist curves, as shown in Fig. 5, are composed of a semicircle (at high frequencies) and a steep straight line (at low frequencies). A comparative analysis of NC and NiO/NiS_2@NC electrodes reveals that the NiO/NiS_2@NC hybrid electrode demonstrates lower charge transfer (R_{ct}=8 Ω) in comparison to NC (R_{ct}=12 Ω), indicating enhancement of electrical conductivity of NiO/NiS_2@NC.

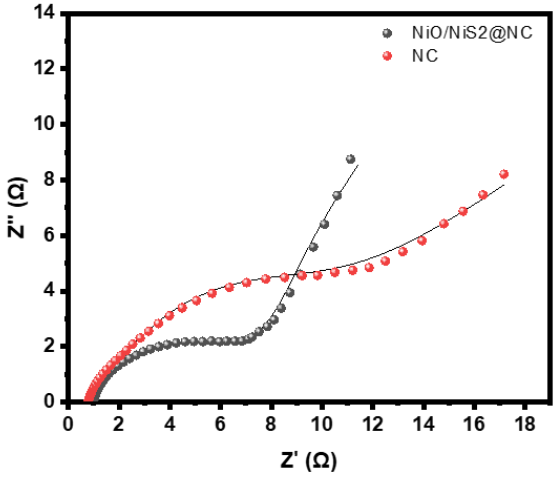

Fig. 5: Nyquist Plot of NC and NiO/NiS_2@NC.

5. Conclusion

In this study, a NiO/NiS_2@NC composite was efficiently synthesized using an effortless procedure. In the heterogeneous structure of the synthesized material NiO/NiS_2@NC derived from PAM, which is abundant with carbon and nitrogen and has unusual gelation characteristics, permitting in-situ reduction of the trapped metal ions during heat treatment. Additionally, N-doped carbon plays a crucial role in enhancing supercapacitor performance by increasing the surface area, specific capacitance, and retention rate. The synergistic interaction between NiS_2, NiO and nitrogen-doped carbon provides further pseudocapacitance and enhances the conductivity of the electrode. Thus, NiO/NiS_2@NC exhibits outstanding performance in supercapacitors, with a specific capacitance of up to 1134 F g^{-1} at 1 A g^{-1} compared to NC, which delivers a specific capacitance of 369 A g^{-1} at the same current density. While the NiO/NiS_2@NC composite demonstrates impressive specific capacitance, there remains a need for further optimization regarding its long-term performance at elevated current densities and in the context of large-scale electrode fabrication. Future efforts will concentrate on enhancing structural stability during prolonged cycling, examining scalable synthesis techniques, and exploring additional heteroatom-doped carbon supports to further improve electrochemical performance.

4. References

1. Pablo-Romero, M. d. P.; Pozo-Barajas, R.; Yñiguez, R., (2017) Global changes in residential energy consumption. Energy Policy**, 101,** 342-352.
2. Kouchachvili, L.; Yaïci, W.; Entchev, E., (2018) Hybrid battery/supercapacitor energy storage system for the electric vehicles. *J Power Sources***, 374**, 237-248.
3. Dubal, D. P.; Ayyad, O.; Ruiz, V.; Gómez-Romero, P., (2015) Hybrid energy storage: the merging of battery and supercapacitor chemistries. Chem Soc Rev**, 44 (7)**, 1777-1790.
4. Liu, H.; Xu, T.; Cai, C.; Liu, K.; Liu, W.; Zhang, M.; Du, H.; Si, C.; Zhang, K., (2022) Multifunctional superelastic, superhydrophilic, and ultralight

nanocellulose-based composite carbon aerogels for compressive supercapacitor and strain sensor. Adv Funct Mater**, 32 (26)**, 2113082.
5. Wang, T.; Xiong, C.; Zhang, Y.; Wang, B.; Xiong, Q.; Zhao, M.; Ni, Y., (2024) Multi-layer hierarchical cellulose nanofibers/carbon nanotubes/vinasse activated carbon composite materials for supercapacitors and electromagnetic interference shielding. Nano Res**, 17** (3), 904-912.
6. Xiang, X.; Zhang, W.; Yang, Z.; Zhang, Y.; Zhang, H.; Zhang, H.; Guo, H.; Zhang, X.; Li, Q., (2016) Smart and flexible supercapacitor based on a porous carbon nanotube film and polyaniline hydrogel. RSC Adv.**, 6 (30)**, 24946-24951.
7. Cao, Z.; Fu, J.; Wu, M.; Hua, T.; Hu, H., (2021) Synchronously manipulating Zn2+ transfer and hydrogen/oxygen evolution kinetics in MXene host electrodes toward symmetric Zn-ions micro-supercapacitor with enhanced areal energy density. Energy Storage Materials**, 40**, 10-21.
8. He, T.; Zhang, W.; Manasa, P.; Ran, F. (2020), Quantum dots of molybdenum nitride embedded in continuously distributed polyaniline as a novel electrode material for supercapacitor. *J Alloys Compd***, 812**, 152138.
9. Tang, Y.; Chen, T.; Yu, S.; Qiao, Y.; Mu, S.; Zhang, S.; Zhao, Y.; Hou, L.; Huang, W.; Gao, F., (2015) A highly electronic conductive cobalt nickel sulphide dendrite/quasi-spherical nanocomposite for a supercapacitor electrode with ultrahigh areal specific capacitance. *J Power Sources***, 295**, 314-322.
10. Zhang, Z.; Wang, Q.; Zhao, C.; Min, S.; Qian, X., (2015) One-step hydrothermal synthesis of 3D petal-like Co_9S_8/RGO/Ni_3S_2 composite on nickel foam for high-performance supercapacitors. ACS Appl Mater Interfaces**, 7 (8**), 4861-4868.
11. Ansari, S. A.; Fouad, H.; Ansari, S. G.; Sk, M. P.; Cho, M. H., (2017) Mechanically exfoliated MoS2 sheet coupled with conductive polyaniline as a superior supercapacitor electrode material. *J Colloid Interface Sci***, 504**, 276-282.
12. Chang, Z.; Ju, X.; Guo, P.; Zhu, X.; Liao, C.; Zong, Y.; Li, X.; Zheng, X., (2020) Enhanced performance of supercapacitor electrode materials based on hierarchical hollow flowerlike HRGOs/Ni-doped MoS2 composite. *J Alloys Compd***, 824,** 153873.
13. Jayakumar, S.; Santhosh, P. C.; Mohideen, M. M.; Radhamani, A. V., (2024) A comprehensive review of metal oxides (RuO2, Co3O4, MnO2 and NiO) for supercapacitor applications and global market trends. *J Alloys Compd***, 976**, 173170.
14. Chime, U. K.; Nkele, A. C.; Ezugwu, S.; Nwanya, A. C.; Shinde, N. M.; Kebede, M.; Ejikeme, P. M.; Maaza, M.; Ezema, F. I., (2020) Recent progress in nickel oxide-based electrodes for high-performance supercapacitors. Curr Opin Electrochem**, 21**, 175-181.
15. Pothu, R.; Bolagam, R.; Wang, Q.-H.; Ni, W.; Cai, J.-F.; Peng, X.-X.; Feng, Y.-Z.; Ma, J.-M., (2021) Nickel sulfide-based energy storage materials for high-performance electrochemical capacitors. Rare Metals**, 40 (2)**, 353-373.
16. Wang, D.-W.; Li, F.; Yin, L.-C.; Lu, X.; Chen, Z.-G.; Gentle, I. R.; Lu, G. Q.; Cheng, H.-M., (2012) Nitrogen-doped carbon monolith for alkaline supercapacitors and understanding nitrogen-induced redox transitions. *Chem. Eur. J***, *18* (17**), 5345-5351.
17. Dai, L.; Chang, D. W.; Baek, J.-B.; Lu, W., (2012) Carbon nanomaterials for advanced energy conversion and storage. Small**, 8 (8)**, 1130-1166.
18. Chen, P.; Wang, L.-K.; Wang, G.; Gao, M.-R.; Ge, J.; Yuan, W.-J.; Shen, Y.-H.; Xie, A.-J.; Yu, S.-H., (2014) Nitrogen-doped nanoporous carbon nanosheets derived from plant biomass: an efficient catalyst for oxygen reduction reaction. Energy Environ. Sci.**, 7 (12)**, 4095-4103.
19. Wei, L.; Sevilla, M.; Fuertes, A. B.; Mokaya, R.; Yushin, G., (2012) Polypyrrole-Derived Activated Carbons for High-Performance Electrical Double-Layer Capacitors with Ionic Liquid

Electrolyte. Adv Funct Mater**, 22 (4)**, 827-834.
20. He, T.; Fu, Y.; Meng, X.; Yu, X.; Wang, X., (2018) A novel strategy for the high performance supercapacitor based on polyacrylonitrile-derived porous nanofibers as electrode and separator in ionic liquid electrolyte. Electrochim Acta**, 282**, 97-104.
21. Wang, S.-j.; Liang, K.; Li, J.-b.; Huang, X.-b.; Ren, Y.-r., (2023) Surfactant-assisted synthesis of self-assembled Na3V2(PO4)2F3@C microspheres as the cathode for Na-ion batteries. Vacuum**, 211**, 111894.
22. Soofivand, F.; Esmaeili, E.; Sabet, M.; Salavati-Niasari, M., (2018) Simple synthesis, characterization and investigation of photocatalytic activity of NiS2 nanoparticles using new precursors by hydrothermal method. *J Mater Sci: Mater Electron**, 29*** **(1**), 858-865.
23. Wang, S.-C.; Xiong, D.; Chen, C.; Gu, M.; Yi, F.-Y., (2020**)** The controlled fabrication of hierarchical CoS2@NiS2 core-shell nanocubes by utilizing prussian blue analogue for enhanced capacitive energy storage performance. *J Power Sources***, 450**, 227712.
24. Liu, Y.; Zhang, H.; Chen, G.; Wang, X.; Qian, Y.; Wu, Z.; You, W.; Tang, Y.; Zhang, J.; Che, R., (2024) Engineering phase to reinforce dielectric polarization in nickel sulfide heterostructure for electromagnetic wave absorption. Small**, 20 (17)**, e2308129.
25. Shombe, G. B.; Khan, M. D.; Zequine, C.; Zhao, C.; Gupta, R. K.; Revaprasadu, N., (2020) Direct solvent free synthesis of bare α-NiS, β-NiS and α-β-NiS composite as excellent electrocatalysts: Effect of self-capping on supercapacitance and overall water splitting activity. Sci Rep**, 10** (**1**), 3260.
26. Deep Yadav, D.; Jha, R.; Singh, S.; Kumar, A., (2023) Synthesis and characterisation of Nickel oxide nanoparticles using CTAB as capping agent. Materials Today: Proceedings**, 73**, 333-336.
27. Radhika, G.; Krishnaveni, K.; Kalaiselvi, C.; Subadevi, R.; Sivakumar, M., (2020) Sway of MnO2 with poly(acrylonitrile) in the sulfur-based electrode for lithium–sulfur batteries. Polym. Bull.**, 77 (8)**, 4167-4179.